



Targeting Serine Protease High-temperature Requirement Factor A1 with Small Molecules Ligands as Potential Therapeutics for Alzheimer's Disease

Jenny Wang

Abstract

Alzheimer's disease, the primary cause of dementia, is rapidly becoming one of the most expensive, burdening, and lethal diseases of the century. The progression of this disease involves the accumulation of beta amyloid fragments forming amyloid plaques which disrupts brain function. The HTRA1 protein has shown promise in the inhibition of amyloid plaque formation and AD development, with studies of HTRA1 exhibiting reduced aggregation of beta amyloid plaques and degraded fibrillar tau which contribute to Alzheimer's. Developing a small molecule ligand of HTRA1 could be useful in regulating the progression of

Alzheimer's disease. Computational methods are used as a cost effective way for a primary investigation of determining potential ligands. HTRA1 was scanned through FPocketWeb, CavityPlus, and PrankWeb for potential ligand binding sites, which were found in promising quantities, warranting further investigation into molecules that would interact with these binding sites. PocketQuery and ZINCPharmer with HTRA1 and a peptide (PBDcode:2JOA) were utilized for a pharmacophore based virtual screening to find 20 hit compounds fitting five pharmacophore maps. To determine the compound with the most favorable interaction with HTRA1, the identified compounds were subject to further screening using SwissDock. The five compounds with the lowest Gibbs free energy values and most favorable interactions were inputted into SwissADME. This was done to analyze drug likeness properties, which showed promising results for three out of five compounds.

Keywords

Alzheimer's disease, Beta amyloid hypothesis, Drug discovery, ligand discovery, HTRA1, Virtual screening, Aging, Dementia

Received 11 Dec., 2024; Revised 20 Dec., 2024; Accepted 23 Dec., 2024 © The author(s) 2024.

Published with open access at www.questjournals.org

I. Introduction

Alzheimer's disease is a neurodegenerative disease that is a growing issue among today's population. It results in the loss of memory, language, problem-solving and other thinking capabilities and is considered the main cause of dementia, a general term describing the impairment of brain function [1]. About 50 million people have dementia worldwide, and this number is predicted to triple, increasing to 152 million globally in 2050, as reported by the World Alzheimer Report 2019 [2]. Alzheimer's disease is more prevalent in individuals over the age of 65, however, in rare cases of early onset Alzheimer's it can affect individuals under 65 [3]. Symptoms are known to worsen over time and eventually interfere with daily tasks [3]. While the disease does not directly cause death, it increases the vulnerability of an individual to other incidents [3]. The cause of Alzheimer's disease is widely believed to be a result of a combination of genetic, lifestyle and environmental factors that affect the brain over time [4]. Possible risk factors contributing to Alzheimer's disease include increasing age, family history and genetics, cardiovascular diseases, and environmental influences such as air pollution [4].

The development of Alzheimer's usually begins with damage to the region of the brain that controls memory, including the entorhinal cortex and hippocampus [5]. The disease then progresses into the cerebral cortex, affecting many behaviors like communication and reasoning [6]. As it eventually reaches and damages other areas of the brain [6]. Recent research on the cause and prevention of Alzheimer's has been focused on the role of amyloid plaques and neurofibrillary tangles that are commonly found in the

brain of Alzheimer's patients [7]. Plaques are abnormal clumps and appear to have a toxic effect on neurons and to disrupt communication between brain cells [8]. They are made of cellular debris and misfolded α -Synuclein (α -syn), a proliferating neuronal protein which assists in regulation of synaptic function, that becomes β -sheet rich amyloid fibrils [9-11]. Neurofibrillary tangles are formed from tau proteins that change shape and organize into structures which disrupt the brain transport system and cause damage to cells [8]. The presence of the amyloid plaques and neurofibrillary tangles are considered the main indicators of AD.

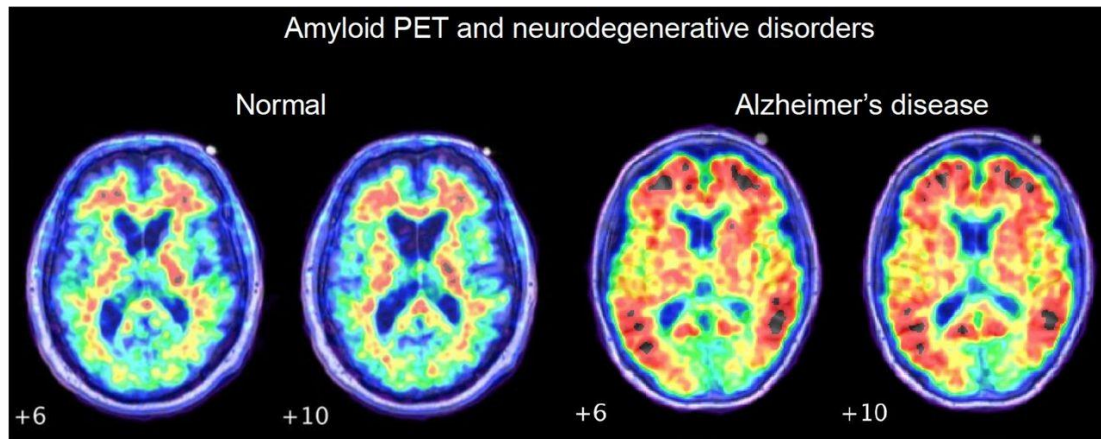


Fig.1 Comparison of Healthy Brain and brain affected by Alzheimer's. The AD brain has significantly more amyloid as a result of the increase in amyloid plaques in the brain [12].

The Amyloid Hypothesis is a possible explanation for the development of AD. It was previously discovered that the beta-amyloid protein is the central component of extracellular amyloid plaques in AD [13]. Since then, the Amyloid Hypothesis, believing that the flaws in the processes governing production, accumulation or disposal of beta-amyloid is the primary cause of Alzheimer's, has become a leading theory of AD pathogenesis [14]. Over the past decades, targeting beta-amyloid protein has been the focus of developing AD treatment [14].

Further evidence for this hypothesis comes from genetic studies that have supported the causative role of beta-amyloid accumulation in AD pathogenesis [14]. Mutations in the genes APP, presenilin 1 (PSEN1) and PSEN2 that increase beta-amyloid formation are shown to promote plaque formation and lead to autosomal dominant early-onset familial AD (FAD) [15, 16]. In addition, Down syndrome (DS) patients have an extra copy of the APP gene, which leads to most patients exhibiting typical AD neuropathology with significant levels of beta-amyloid plaques and tangles by age 40 [17-19]. On the other hand, a mutation in the APP gene in Icelandic populations reduces beta-amyloid production, which is shown to reduce the risk of dementia in the population [20]. Both genetic and non-genetic risk factors for late-onset Alzheimer's (SAD) have been found to affect beta-amyloid production [14]. Beta-amyloid's involvement in AD progression supports the motivation of Alzheimer research to pursue anti-beta-amyloid therapies. While failures have occurred in the targeting of beta-amyloid, recent developments on anti-beta-amyloid therapies have shown further progress [14]. Recently, Aducanumab and Lecanemab, both therapeutic targeting $A\beta$ aggregation, obtained

FDA-approval [21, 22]. These drugs have seen positive results in slowing the progression of AD, displaying promise that targeting amyloid plaques can successfully result in modification of disease progression [23].

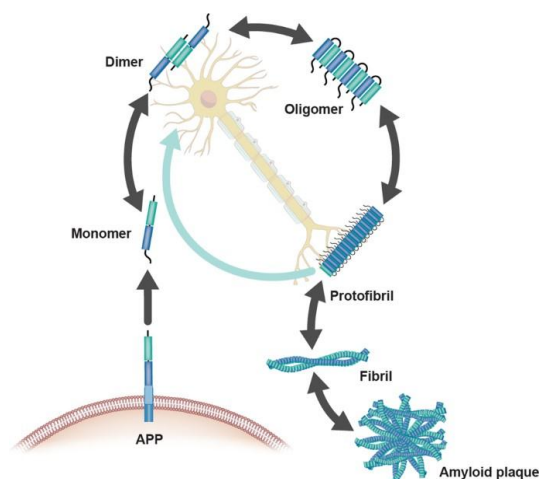


Fig.2 Illustration of aggregation in the brain from beta-amyloid monomers to form an Amyloid plaque [24]. The monomers are shown to be generated from the APP gene, with an extracopy in DS patients causing an increase in Amyloid plaques [17-19].

HTRA1 is a promising target gene for inhibiting amyloid plaque formation and AD development. HTRA1, known as high-temperature requirement factor A1 (HTRA1), is a serine protease, an enzyme responsible for breaking down other proteins. The protein is ATP-independent with a PDZ domain [25]. HTRA1 and its isoforms are found in bacteria, fungi, plants, and animals and function in the stress response by binding from its PDZ domain to damaged proteins to break them down [26,27]. The protein is found throughout the extracellular matrix and is found in the cytoplasm and nucleus intracellularly [23,28]. PDZ domain proteins are known to bind to substrates containing β -sheets, which suggests it may bind to β -sheet-rich amyloid species present in AD [23].

Other studies support this prediction, suggesting that HTRA1 may be involved in the reduced aggregation of beta amyloid plaques, and alterations in HTRA1 activity could impact the buildup of these plaques [23,29]. Amyloid and other misfolded proteins are seen to be highly resistant

to degradation and currently without therapeutic stores to remove misfolded proteins; however, HTRA1 was found to degrade amyloid fibril aggregates [23,30]. Developing a drug to regulate HTRA1 expression would be beneficial in an attempt to inhibit AD development. The goal of this project is to determine small molecule ligands of HTRA1 which can serve as the starting point for future development of AD treatment targeting amyloid plaques.

1. Materials and Methods

1.1. Analysis of binding sites in HTRA1:

In the first experiment, three tools were used to determine viable ligand binding sites on HTRA1, including CavityPlus (<http://www.pkumdl.cn:8000/cavityplus/index.php#/>), FPocketWeb (<https://durrantlab.pitt.edu/fpocketweb/>), and PrankWeb (<https://prankweb.cz/>). The PDB code 3TJN was used in each of these programs. This PDB code is of the unbound protein HTRA1 without additional molecules.

1.1.1 CavityPlus

Using CavityPlus (<http://www.pkumdl.cn:8000/cavityplus/index.php#/>) and inputting the PDB code 3TJN, then select in g chains A, B, and D and pressing "Submit" yields the results. The default settings are kept for the other parts of the program. Google sheets were used to generate the data table based on the results from CavityPlus.

1.1.2 FPocketWeb

Using FPocketWeb (<https://durrantlab.pitt.edu/fpocketweb/>) and inputting the PDB code 3TJN, proceed to press "Load" then "Start" FPocketWeb" which yields the results. Ensure that chains A, B, and D are selected on the first page before pressing "Start FPocketWeb." The default settings are kept for the other parts of the program. Google sheets were used to generate the data table based on the results

Its from FPocketWeb.

1.1.3 PrankWeb

Using PrankWeb (<https://prankweb.cz/>) and inputting the PDB code 3TJN, then pressing submit yields the results. The default settings are kept for other parts of the program. Google sheets were used to generate the data table based on the results from PrankWeb.

2.2 Pharmacophore map using PocketQuery

PocketQuery (<http://pocketquery.csb.pitt.edu/>) was used to generate pharmacophore maps of HTRA1. Entering the PDB code 2JOA yielded the results in the data table and figures. Five clusters were selected based on if the clusters were chain B and highest score.

2.3 Molecule identification utilizing ZINCPharmer

The top five clusters identified by PocketQuery were exported to ZINCPharmer (<http://zincpharmer.csb.pitt.edu/>) to produce the results. In cluster two through five, some of the duplicate pharmacophore elements were removed to where each cluster had four interactions remaining. This was to ensure there was a reliable number of hit molecules below RMSD.4 to conduct further studies. Four molecules from each cluster were selected based on the lowest RMSD value by clicking RMSD twice.

2.4 Molecular docking with SwissDock

The binding ability of the compounds previously identified by ZINCPharmer to HTRA1 was observed using SwissDock (<http://old.swissdock.ch/docking>). HTRA1 (PDB code: 3TJN) was uploaded as the target selection. The twenty ZINC codes of compounds previously by ZINCPharmer were inputted for ligand selection. Two of the twenty ZINC codes were repeated, resulting in SwissDock being run 18 times. If the ZINC code was recognized by SwissDock, the ligand was selected and designated to "Dock selected ligand." If the ZINC code was not recognized by SwissDock, a file of the compound was obtained through OPENBABEL (<https://www.cheminfo.org/Chemistry/Cheminformatics/FormatConverter/index.html>) by converting the

2.5 Drug Likeness prediction by SwissADME

Drug likeness properties were analyzed by SwissADME (<http://www.swissadme.ch/>). A SMILE code was entered for each of the top 5 compounds identified by SwissDock. The SMILE code was obtained using ZINC12 (<https://zinc12.docking.org/>) by entering the ZINC code into the search bar. After the SMILE code was inputted, RUN was pressed on default settings. Molecular Weight (g/mol), Num. H-bond acceptors, Num. H-bond donors, LogPo/w (iLOGP), Lipinski, Violations, Water Solubility LogS (ESOL) Class, GI absorption, and BBB permeant properties were recorded in the data table.

2. Results and Discussion

3.1 Analysis of potential ligand binding sites

The first experiment is focused on determining binding sites for small molecules in proteins. This is crucial as the availability of such binding sites for small molecules will allow for further studies to identify smaller molecules that bind to the protein. From the three programs used to determine binding sites, over fifty possible binding sites were found.

3.1.1 CavityPlus

As a first approach to find such binding sites, CavityPlus is used, which is a geometric based method considering the structure of the site to determine a Cavity score for the site [31]. It then utilizes this score to quantitatively determine a site's druggability, showing if a site is suitable for binding drug-like molecules [31]. The results of CavityPlus predict 23 possible ligand binding sites (Fig. 3), with five prospective binding sites having strong and medium druggability and drug score. The binding site with the highest drug score (blue) is significantly larger than the others with a score of 2768, over two times the second highest drug score.

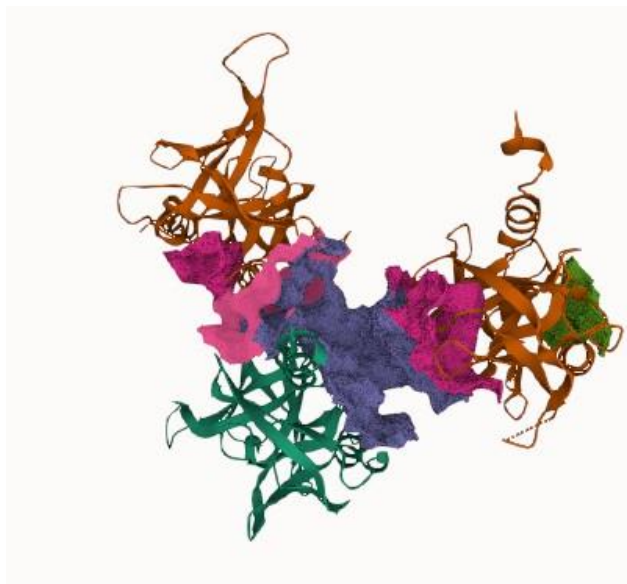


Fig.3 Generated image of HTRA1 using CavityPlus showing select binding sites (PDBID:3TJN). The figures show four Strong and one Medium predicted binding sites and are highlighted in green, magenta, pink, and blue.

Table 1. DrugScore and Druggability of first 10 binding sites by CavityPlus

# ↑↓	DrugScore ↑↓	Druggability ↑↓
1	2768	Strong
2	1011	Strong
3	1339	Strong
4	907	Strong
5	-842	Weak
6	153	Medium
7	-273	Weak
8	-874	Weak
9	-563	Weak
10	-1085	Weak

3.1.2 FPocketWeb

FPocketWeb is a website that runs the program fpocket3 [32]. It is one of the few programs that consider an energy-based approach to identify possible ligand binding sites with energetically favorable conditions [33]. This program resulted in 43 possible binding sites, with 5 ligand binding sites over .1 druggability. Out of these sites, pocket number 43 had the highest druggability, more than two times the druggability of the next highest druggability.

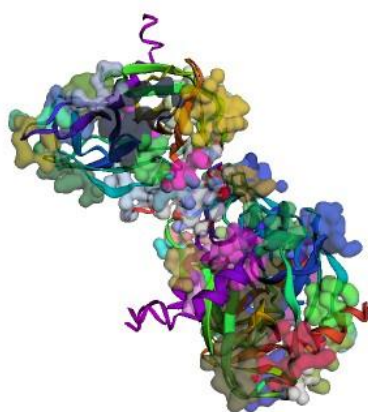


Fig.4Illustrationof43predictedbindingsitesbyFPocketWeb(PDBID:3TJN).

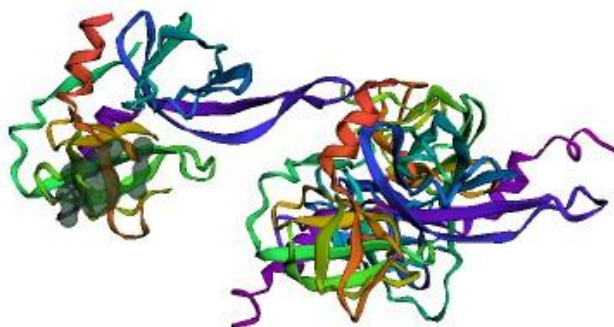


Fig.5 Image of pocket #29 with the highest druggability score. Generated by FPocketWeb (PDBID:3TJN).

Table 2. Table of top 5 binding sites on FPocketWeb based on druggability over 0.1

PocketNumber	Druggability	Score	Volume
29	0.582	-0.017	314.663
16	0.238	0.046	393.467
28	0.177	-0.015	481.56
6	0.114	0.134	321.631
2	0.107	0.182	690.074

3.1.3 PrankWeb

PrankWeb was used to determine potential binding sites. PrankWeb is the online interface for the program P2Rank, a machine learning-based method for determining ligand binding sites [34]. It is shown to predict novel sites due to its template-free method, allowing it to discover new possible protein-ligand complexes [35]. Out of the 5 binding sites, there are three prospective binding sites with scores above three. Out of these three, the score of the first binding site (red) is significantly higher than the other ones, 13.47 compared to 3.7. PrankWeb, FPocketWeb, and CavityPlus all yielded promising results with abundant prospective binding sites for further investigation of targeting HTRA1 for inhibiting amyloid production using ligands.

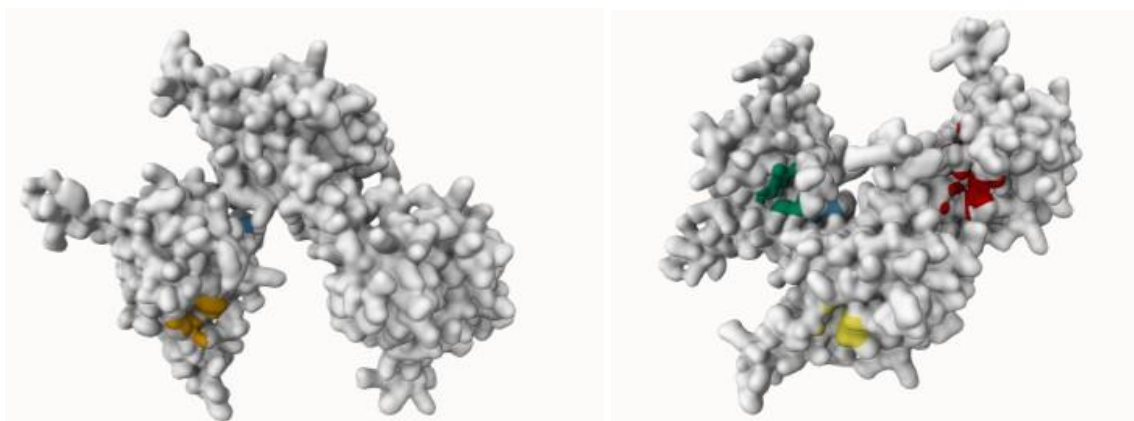


Fig.6 Predicted binding sites of HTRA1 by PrankWeb (PDBID:3TJN). Binding sites are highlighted in green, red, yellow, dark yellow, and blue.

Table 3. Results of the 5 binding sites found by PrankWeb

Rank	Score	Probability
1	13.47	0.706
2	3.7	0.147
3	3.51	0.133
4	1.62	0.025
5	1.13	0.01

3.2 Virtual Screening

These second experiment entailed determining suitable small molecules that could bind to HTRA1. The PDB code 2JOA was used and it consisted of HTRA1 and a peptide. The binding sites of the peptide to HTRA1 were observed using PocketQuery and through ZINCPharmer, 20 small molecules were identified as possible ligands.

3.2.1 map using PocketQuery

Pharmacophore maps were generated using Pocketquery and the five maps with the highest score were selected for further analysis. Pocketquery is an online interface that observes the properties of protein-protein interaction (PPI) for the purpose of drug discovery [36]. It identifies potential binding sites through a given drugability score [36]. The drugability score of the

cluster represents its ability to form interactions with a small molecule inhibitor [36]. The score is on a scale of 0-1. A score of over 0.85 indicating good druggability and a possible binding site of HTRA1. The top 5 clusters with the highest scores all have scores above 0.85, and thus was further investigated using ZINC Pharmer. Visual illustrations of the clusters and their interactions are shown below (Fig.7).

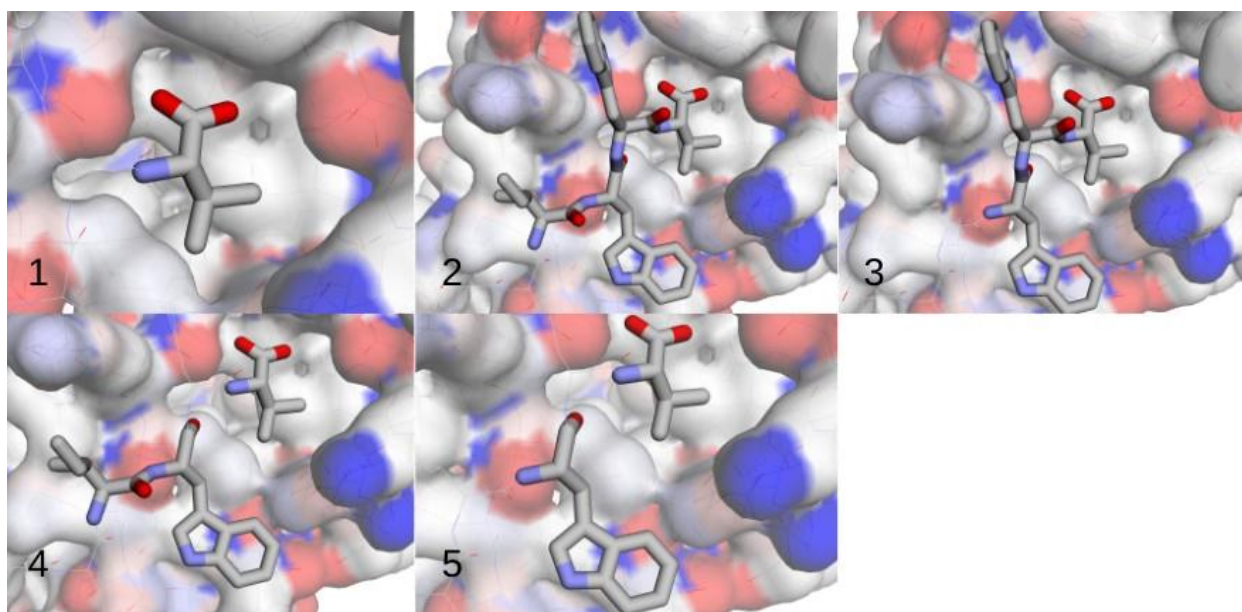


Fig.7 Pocket Query generated Pharmacophore map of HTRA1 bound to a peptide (PDBID:2JOA)

Table 4. Results of the top 5 clusters ranked by score (PDBID:2JOA)

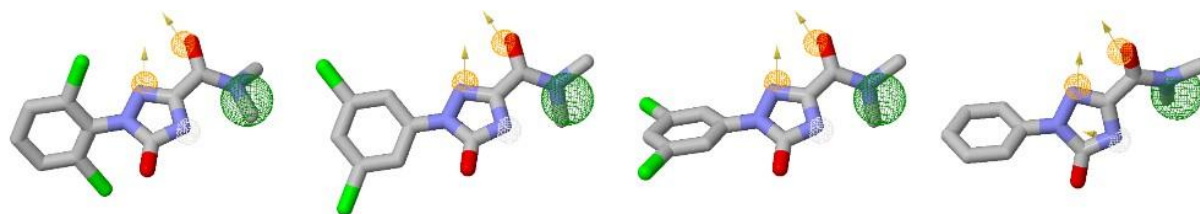
Cluster#	Score	Residue	Residue#	Size	Distance	Chain
1	0.898084	VAL	7	1	0	B
2	0.884624	ILE TRP TRP VAL	4 5 6 7	4	9.5778	B
3	0.872467	TRP TRP VAL	5 6 7	3	8.8039	B

4	0.867201	ILET RPVAL	4 5 7	3	9.5778	B
5	0.859819	TRPVAL	5 7	2	6.8737	B

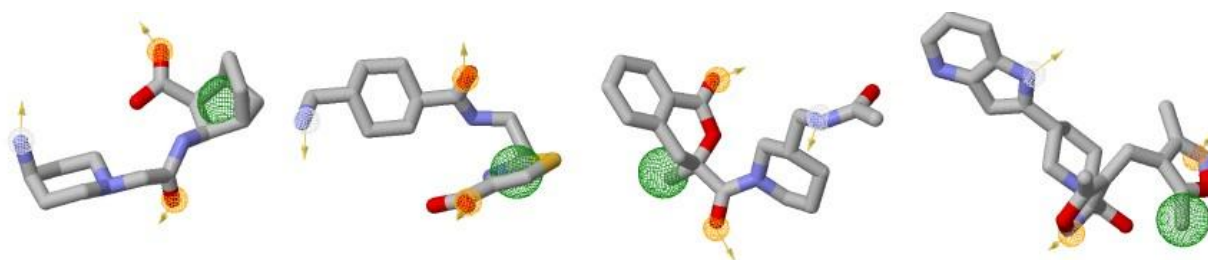
3.2.2 Molecule identification

The top 5 clusters from PocketQuery were exported to ZINCPharmer. ZINCPharmer is a web interface that identifies purchasable compounds which align with a specific pharmacophore map [37]. ZINCPharmer quantifies the alignment between the molecule and the cluster through Root Mean Square Deviation or RMSD. Compounds with lower RMSD have a better geometric match to the pharmacophore [37]. 4 compounds from each cluster were chosen for further investigation based on Root Mean Square Deviation or RMSD value. ZINCPharmer includes different conformers when determining possible ligands, resulting in two repeat ZINC codes for a total of 18 compounds.

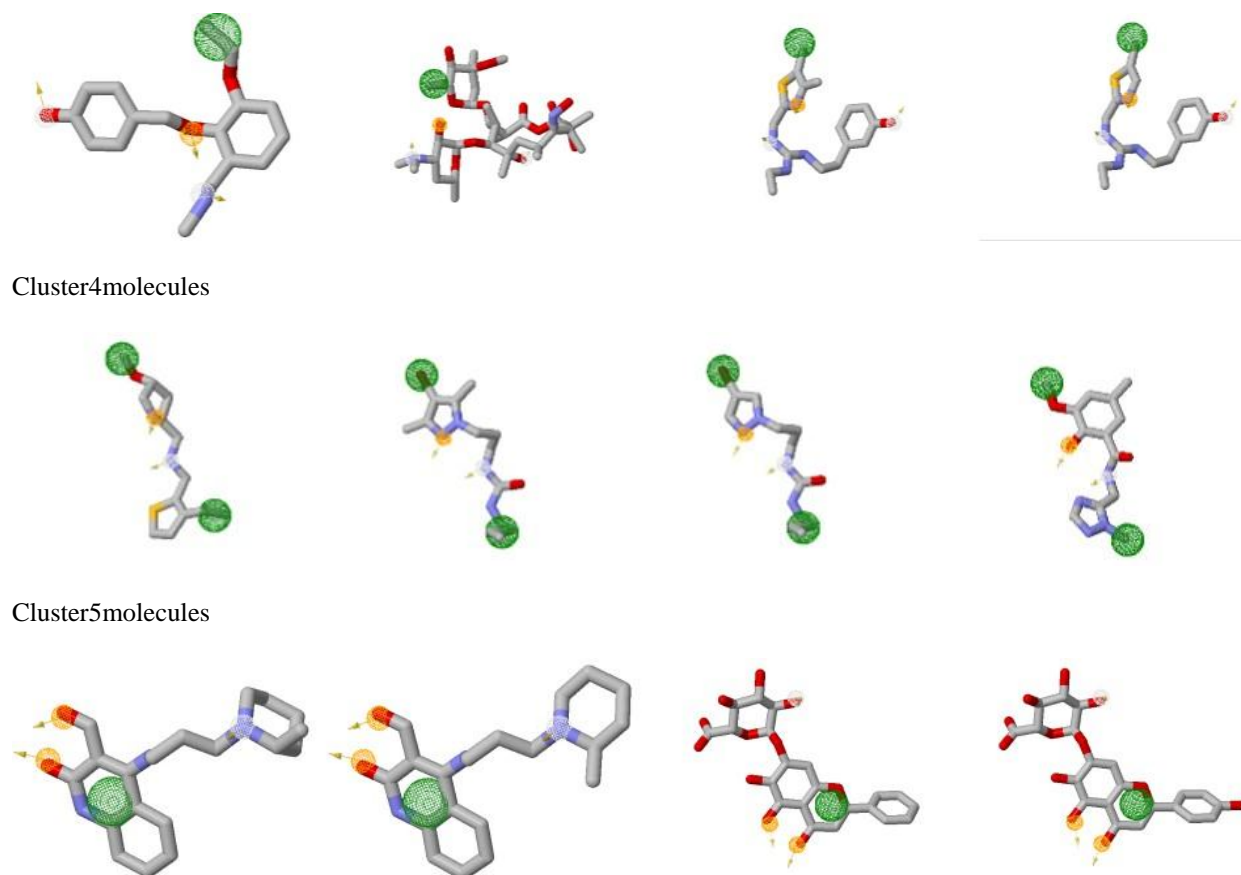
Cluster 1 molecules



Cluster 2 molecules



Cluster 3 molecules



Cluster4molecules

Cluster5molecules

Fig.820smallmoleculesidentifiedby ZINCPharmer. The pharmacophoremap interactions are represented by Green, hydrophobic, yellow, hydrogen acceptor, and white, hydrogen donor.

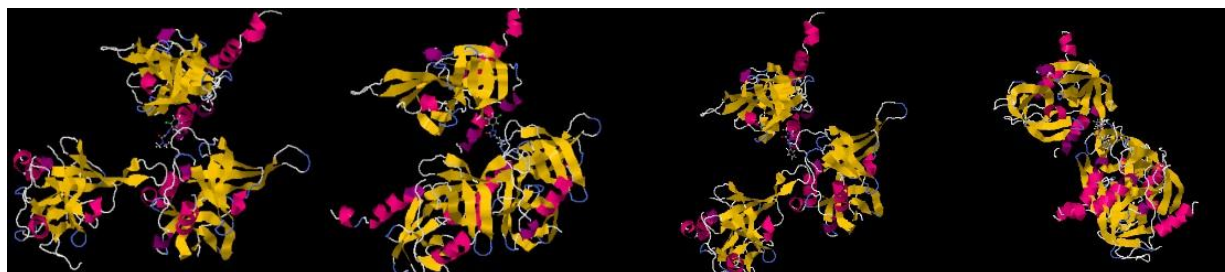
Table5.Detailsofthetop4moleculesofeachclusterbasedonRMSD

Cluster#	Name	RMSD	Mass	RBnds
1	ZINC36533601	0.353	301	5
	ZINC15444140	0.353	301	5
	ZINC15444140	0.353	301	5
	ZINC15444133	0.354	232	5
2	ZINC92715070	0.151	295	4
	ZINC93426091	0.215	311	6
	ZINC67363835	0.282	344	5
	ZINC19580940	0.282	419	8

3	ZINC94679710	0.293	288	10
	ZINC85893874	0.304	750	15
	ZINC85444486	0.328	333	12
	ZINC81188012	0.331	319	11
4	ZINC94879818	0.147	255	8
	ZINC27928090	0.152	331	8
	ZINC27928791	0.155	303	6
	ZINC75487197	0.158	276	7
5	ZINC06681836	0.289	328	7
	ZINC06681836	0.289	328	7
	ZINC34114798	0.297	445	9
	ZINC21992914	0.297	461	10

3.3 Molecular Docking

Molecular docking was used to determine the favorability of the identified compounds from PocketQuery as ligands to HTRA1. This was done through SwissDock, a web server that simulates protein-ligand docking based on the program EADockDSS [38]. The results showed that there were multiple locations/pockets where the ligand could bind. There were also multiple conformations that the ligand could be presented. The location and conformation could impact the ΔG value of the interaction. The lowest ΔG value considering the location and conformation from each simulated protein-ligand interaction was recorded in the table. A lower or more negative ΔG value correlates to a more favorable protein-ligand interaction which means that the ligand has a higher binding ability to the protein.

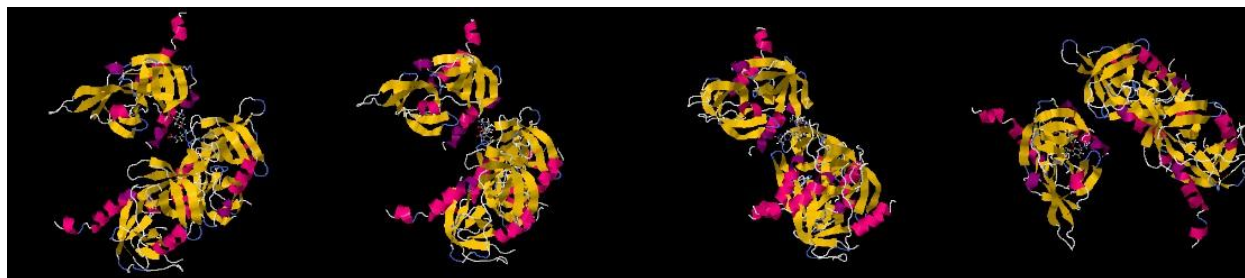


ZINC36533601

ZINC15444140

ZINC15444133

ZINC92715070

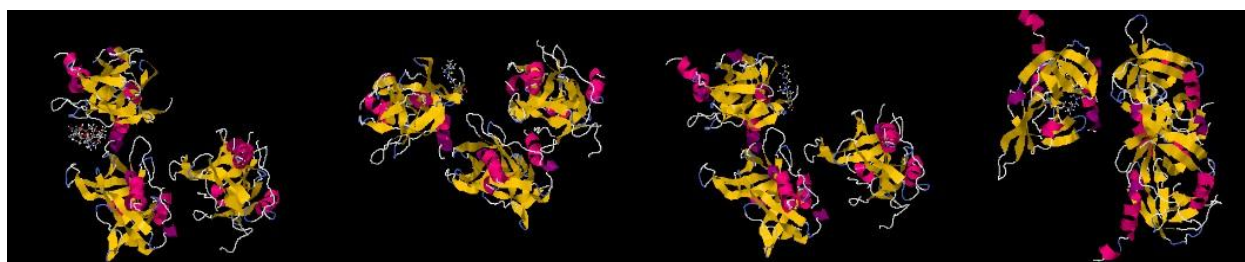


ZINC93426091

ZINC67363835

ZINC19580940

ZINC94679710



ZINC85893874

ZINC85444486

ZINC81188012

ZINC94879818



ZINC27928090

ZINC27928791

ZINC75487197

ZINC06681836



ZINC34114798ZINC21992914

Fig.9 ModelsofinteractionsbetweencompoundsidentifiedbyPocketQueryandbindingsiteofHTRA1usingSwiss Dock (PDBID:3TJN)

Table6. ΔG valuesofinteractionsbetweencompoundsidentifiedbyPocketQueryandbindingsiteofHTRA1using SwissDockcomparingbindingfavorability(PDB ID:3TJN)

Molecule	Numberof bindingsites	Estimated ΔG (kcal/mol)
ZINC36533601	50	-9.64
ZINC15444140	37	-8.58
ZINC15444133	48	-9.06
ZINC92715070	43	-9.37
ZINC93426091	49	-10.77
ZINC67363835	48	-7.95
ZINC19580940	37	-8.16
ZINC94679710	35	-8.12
ZINC85893874	31	-8.74
ZINC85444486	42	-7.98
ZINC81188012	36	-8.39
ZINC94879818	40	-7.94

ZINC27928090	47	-9.68
ZINC27928791	40	-8.07
ZINC75487197	42	-8.62
ZINC06681836	47	-8.47
ZINC34114798	39	-10.62
ZINC21992914	32	-11.13

Out of the 18 hit molecules, the top 5 molecules with the lowest ΔG value and the highest binding ability had estimated ΔG (kcal/mol) of -11.13, -10.77, -10.62, -9.68, -9.64. The number of possible binding sites was shown to have little impact on the estimated ΔG value.

Table 7. Top 5 molecules with most favorable interactions

Molecule	Number of binding sites	Estimated ΔG (kcal/mol)
ZINC21992914	32	-11.13
ZINC93426091	49	-10.77
ZINC34114798	39	-10.62
ZINC27928090	47	-9.68
ZINC36533601	50	-9.64

3.4 SwissADME Drug Likeness

Five selected ligands based on SwissDock were inputted into SwissADME to determine their theoretical drug likeness properties for the goal of deciding whether they would be viable small molecule drugs. SwissADME (<http://www.swissadme.ch/>) is a website that takes a SMILE code or drawn chemical structure and predicts its physicochemical properties, pharmacokinetics, drug-likeness and medicinal chemistry friendliness, estimating the success rate of the molecule as a drug [39]. The results of SwissADME are shown in Table 8. Three compounds, ZINC93426091, ZINC27928090, and ZINC36533601, were shown to follow Lipinski's rule. When drugs are taken orally, the drug has to remain in the body in sufficient concentration to bind to the target and achieve the desired effect. The drug has to remain in the body through

the processes of absorption, distribution, metabolism, and excretion. Lipinski's rule helps to predict this, requiring that the number of hydrogen-bond acceptors ≤ 10 , number of hydrogen-bond donors ≤ 5 , molecular weight ≤ 500 g/mol, and calculated LogP (cLogP) ≤ 5 for sufficient absorption of the drug [40]. Interestingly, ZINC21992914 with the lowest change in Gibbs free energy did not follow Lipinski's rule. Water Solubility and GI absorption is also an important factor in predicting drug likeness, with the molecule being preferably at least moderately soluble in water and high GI absorption. The five compounds all meet the requirement for water solubility. ZINC27928090 and ZINC36533601 seem promising, fulfilling the qualifications for a potential drug in Lipinski, water solubility, and GI absorption. In addition, both molecules are blood brain barrier (BBB) permeant, which is estimated to appear in only 2% of small molecule drugs [41]. This is crucial for potential HTRA1 ligands as the protein resides within the BBB. While molecules can be modified to increase BBB permeability, this would shorten the drug synthesis process, making these molecules more advantageous.

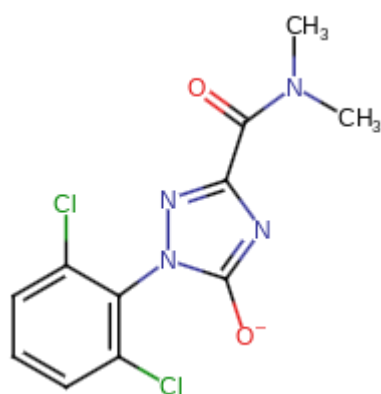


Fig.10 Chemical structure of one of the top compounds for drug likeness, ZINC36533601.

Table 8. SwissADME generated drug likeness properties of the top 5 ligands with the lowest ΔG value

ZINCID	Molecular Weight (g/mol)	Num. H-bond acceptors	Num. H-bond donors	LogPo/w (iLOGP)	Lipinski	Violations	Water Solubility or LogS (ESOL) Class	GI absorption	BBB permeant
ZINC2199	461.35	12	6	1.98	No	2	Soluble	Low	No

2914									
ZINC93426091	311.4	4	2	1.67	Yes	0	VerySoluble	Low	No
ZINC34114798	445.35	11	5	1.86	No	1	Soluble	Low	No
ZINC27928090	331.25	2	2	2.6	Yes	0	Soluble	High	Yes
ZINC36533601	300.12	4	0	2.25	Yes	0	Soluble	High	Yes

4. Conclusion

Alzheimer's disease is one of the most rapidly expanding diseases, with estimates predicting that the affected population will triple to about 152 million people globally with dementia in 2050, with Alzheimer's contributing to 60–70% of cases. The major indicators of AD are the formation of amyloid plaques and neurofibrillary tangles, which inhibit brain functions. Preventing the build up of amyloid fragments and formation of amyloid plaques to inhibit AD development has been the focus of the Amyloid Hypothesis and AD drug development in recent years. The HTRA1 protein has shown promise in achieving this goal, with studies showing its correlation of reduced amyloid aggregation and its ability to degrade fibrillar tau, which is also associated with AD. HTRA1 was first screened for potential binding sites using PrankWeb, FPocketWeb, and CavityPlus, with 5 from PrankWeb, 43 from FPocketWeb, and 23 from CavityPlus, with more than one binding site from each program showing promising druggability results. Warranting further study to identify possible ligands, the second screening involved PocketQuery conducting a pharmacophore-based virtual screening analyzing the druggability of binding sites of HTRA1 to a protein (PDB code: 2JOA). 5 pharmacophore maps with a score of over 0.85 were then inputted into ZINCPharmer generating 20 compounds. SwissDock then determined the Gibbs free energy of the identified compounds binding to HTRA1, with ZINC21992914, ZINC93426091, ZINC34114798, ZINC27928090, ZINC36533601 having the lowest Gibbs free energy values and most favorable interactions. These compounds were then screened by SwissADME, finding that ZINC93426091, ZINC27928090, ZINC36533601 follow Lipinski's rule and show promising drug-likeness properties. Interestingly, ZINC21992914 with the most favorable interaction did not follow Lipinski's rule.

Limitations to this study are that results are theoretically calculated using computer programs and have not been verified physically. In addition, the RMSD values for compounds in the first cluster were higher than recommended being over 0.35. There has also been a limited quantity of compounds taken from ZINCPharmer while there were more molecules that met the above 1.35 mark due to the limited number of people working on this project. This project can be taken further by physical screening of the final compounds, testing if they successfully bind to HTRA1 in a real setting. Further objectives if physical screening is successful could be testing the small molecule drugs in animal models.



Research Paper

Acknowledgements

I am incredibly thankful to my mentor, Dr. Moustafa Gabr, for assisting me in this project. His guidance was crucial in my success, suggesting the direction for the research topic and providing resources for the project. He helped me find a few initial research papers on HTRA1 and directed me to the programs CavityPlus, Fpocketweb, Prankweb, PocketQuery, ZINCPharmer, SwissDock, and SwissADME to run experiments. When I had questions or issues about the research or research process, he provided guidance and helped me to overcome these difficulties. Finally, he peer-reviewed and gave feedback on the final draft of the research paper.

References

- Scheltens P, De Strooper B, Kivipelto M, Holstege H, Chételat G, Teunissen CE, Cummings J, Vander Flier WM. Alzheimer's disease. *Lancet*. 2021 Apr 24;397(10284):1577-1590. doi:10.1016/S0140-6736(20)32205-4. Epub 2021 Mar 2. PMID:33667416; PMCID:PMC8354300.
- James BD, Bennett DA. Causes and Patterns of Dementia: An Update in the Era of Redefining Alzheimer's Disease. *Annu Rev Public Health*. 2019 Apr 1;40:65-84. doi:10.1146/annurev-publhealth-040218-043758. Epub 2019 Jan 14. PMID:30642228.
- Kumar A. Alzheimer disease [Internet]. U.S. National Library of Medicine; 2024 [cited 2024 Aug 18]. Available from: <https://www.ncbi.nlm.nih.gov/books/NBK499922/>
- Breijyeh Z, Karaman R. Comprehensive review on Alzheimer's disease: Causes and treatment. *Molecules* [Internet]. 2020 Dec 8;25(24):5789. Available from: <https://www.mdpi.com/1420-3049/25/24/5789>
- Igarashi KM. Entorhinal cortex dysfunction in Alzheimer's disease. *Trends Neurosci*. 2023 Feb;46(2):124-136. doi:10.1016/j.tins.2022.11.006. Epub 2022 Dec 10. PMID:36513524; PMCID:PMC9877178.
- Fjell AM, McEvoy L, Holland D, Dale AM, Walhovd KB; Alzheimer's Disease Neuroimaging Initiative. What is normal in normal aging? Effects of aging, amyloid and Alzheimer's disease on the cerebral cortex and the hippocampus. *Prog Neurobiol*. 2014 Jun;117:20-40. doi:10.1016/j.pneurobio.2014.02.004. Epub 2014 Feb 16. PMID:24548606; PMCID:PMC4343307.
- O'Brien RJ, Wong PC. Amyloid precursor protein processing and Alzheimer's disease. *Annu Rev Neurosci*. 2011;34:185-204. doi:10.1146/annurev-neuro-061010-113613. PMID:21456963; PMCID:PMC3174086.
- Alzheimer's Disease NHS [Internet]. 2024 [cited 2024 Aug 18]. Available from: <https://www.nhs.uk/conditions/alzheimers-disease/#:~:text=Who%20is%20affected%3F,over%20the%20age%20of%2080>
- Forman MS, Trojanowski JQ, Lee VM. Neurodegenerative diseases: a decade of discoveries paves the way for therapeutic breakthroughs. *Nat Med*. 2004 Oct;10(10):1055-63. doi:10.1038/nm1113. PMID:15459709.
- Oliveira LMA, Gasser T, Edwards R, Zweckstetter M, Melki R, Stefanis L, Lashuel HA, Sulzer D, Vekrellis K, Halliday GM, Tomlinson JJ, Schlossmacher M, Jensen PH, Schulze-Hentrich J, Riess O, Hirst WD, El-Agnaf O, Mollenhauer B, Lansbury P, Outeiro TF. Alpha-synuclein research: defining strategic moves in the battle against Parkinson's disease. *NPJ Parkinsons Dis*. 2021 Jul 26;7(1):65. doi:10.1038/s41531-021-00203-9. PMID:34312398; PMCID:PMC8313662.
- Dobson CM. Protein folding and misfolding. *Nature*. 2003 Dec 18;426(6968):884-90. doi:10.1038/nature02261. PMID:14685248.
- Chapleau M, Iaccarino L, Soleimani-Meigooni D, Rabinovici GD. The role of amyloid PET in imaging neurodegenerative disorders: a review. *Journal of Nuclear Medicine* [Internet]. 2022 Jun 1;63(Supplement 1):13S-19S. Available from: https://jnm.snmjournals.org/content/63/Supplement_1/13S
- Glennner GG, Wong CW. Alzheimer's disease: initial report of the purification and characterization of a novel cerebrovascular amyloid protein. *Biochem Biophys Res Commun*. 1984 May 16;120(3):885-90. doi:10.1016/s0006-291x(84)80190-4. PMID:6375662.
- Zhang Y, Chen H, Li R, Sterling K, Song W. Amyloid β -based therapy for Alzheimer's disease: challenges, successes and future. *Signal Transduct Target Ther*. 2023 Jun 30;8(1):248. doi:10.1038/s41392-023-01484-7. PMID:37386015; PMCID:PMC10310781.
- Goate A, Chartier-Harlin MC, Mullan M, Brown J, Crawford F, Fidani L, Giuffra L, Haynes A, Irving N, James L, et al. Segregation of a missense mutation in the amyloid precursor protein gene with familial Alzheimer's disease. *Nature*. 1991 Feb 21;349(6311):704-6. doi:10.1038/349704a0. PMID:1671712.
- Xiao X, Liu H, Liu X, Zhang W, Zhang S, Jiao B. APP, PSEN1, and PSEN2 Variants in Alzheimer's Disease: Systematic Re-evaluation According to ACMG Guidelines. *Front Aging Neurosci*. 2021 Jun 18;13:695808. doi:10.3389/fnagi.2021.695808. PMID:34220489; PMCID:PMC8249733.
- Glennner GG, Wong CW. Alzheimer's disease and Down's syndrome: sharing of a unique cerebrovascular amyloid fibril protein. *Biochem Biophys Res Commun*. 1984 Aug 16;122(3):1131-5. doi:10.1016/0006-291x(84)91209-9. PMID:6236805.
- Burger PC, Vogel FS. The development of the pathologic changes of Alzheimer's disease and senile dementia in patients with Down's syndrome. *Am J Pathol*. 1973 Nov;73(2):457-76. PMID:4271339; PMCID:PMC1904076.
- Head E, Lott IT, Wilcock DM, Lemere CA. Aging in Down Syndrome and the Development of Alzheimer's Disease Neuropathology. *Curr Alzheimer Res*. 2016;13(1):18-29. doi:10.2174/1567205012666151020114607. PMID:26651341; PMCID:PMC4948181.
- Jonsson T, Atwal JK, Steinberg S, Snaedal J, Jonsson PV, Bjornsson S, Stefansson H, Sulem P, Gudbjartsson D, Maloney J, Hoyte K, Gustafson A, Liu Y, Lu Y, Bhangale T, Graham RR, Huttenlocher J, Bjornsdottir G, Andreassen OA, Jonsson EG, Palotie A, Behrens TW, Magnusson OT, Kong A, Thorsteinsdottir U, Watts RJ, Stefansson K. A mutation in APP

protects against Alzheimer's disease and age-related cognitive decline. *Nature*. 2012 Aug 2;488(7409):96-9. doi:10.1038/nature11283.

PMID:22801501.

21. DunnB,SteinP,CavazzoniP.ApprovalofAducanumabforAlzheimerDisease-TheFDA'sPerspective.JAMAIternMed.2021Oct1;181(10):1276-1278.doi:10.1001/jamainternmed.2021.4607.PMID:34254984.
22. vanDyckCH,SwansonCJ,AisenP,BatemanRJ,ChenC,GeeM,KanekiyoM,LiD,ReydermanL,CohenS,FroelichL,KatayamaS,SabbaghM,VellasB,WatsonD,DhaddaS,IrizarryM,KramerLD,IwatsuboT.LecanemabinEarlyAlzheimer'sDisease.NEngJMed.2023Jan5;388(1):9-21.doi:10.1056/NEJMoa2212948.Epub2022Nov29.PMID:36449413.
23. ChenS,PuriA,BellB,FritscheJ,PalaciosHH,BalchM,SprungerML,HowardMK,RyanJJ,HainesJN,PattiGJ,DavisAA,JackrelME.HTRA1disaggregates α -synucleinamyloidfibrilsandconvertsthemintonontoxicandseedingincompetentspecies.NatCommun.2024Mar18;15(1):2436.doi:10.1038/s41467-024-46538-8.PMID:38499535;PMCID:PMC10948756.
24. HampelH,HardyJ,BlennowK,ChenC,PerryG,KimSH,VillemagneVL,AisenP,VendruscoloM,IwatsuboT,MastersCL,ChoM,LannfeltL,CummingsJL,VergalloA.TheAmyloid- β PathwayinAlzheimer'sDisease.MolPsychiatry.2021Oct;26(10):5481-5503.doi:10.1038/s41380-021-01249-0.Epub2021Aug30.PMID:34456336;PMCID:PMC8758495.
25. VandeWalleL,LamkanfiM,VandenabeeleP.ThemitochondrialserineproteaseHtrA2/Omi:anoverview.CellDeathDiffer.2008Mar;15(3):453-60.doi:10.1038/sj.cdd.4402291.Epub2008Jan4.PMID:18174901.
26. PoepselsS,SprengelA,SaccaB,KaschaniF,KaiserM,GatsogiannisC,RaunserS,ClausenT,EhrmannM.DeterminantsofamyloidfibrildegradationbythePDZproteaseHTRA1.NatChemBiol.2015Nov;11(11):862-9.doi:10.1038/nchembio.1931.Epub2015Oct5.PMID:26436840.
27. KrojerT,PangerlK,KurtJ,SawaJ,StinglC,MechtlerK,HuberR,EhrmannM,ClausenT.InterplayofPDZandproteasedomainsofDegPensuresefficienteliminationofmisfoldedproteins.ProcNatAcadSciUSA.2008Jun3;105(22):7702-7.doi:10.1073/pnas.0803392105.Epub2008May27.PMID:18505836;PMCID:PMC2396557.
28. ClausenT,KaiserM,HuberR,EhrmannM.HTRAproteases:regulatedproteolysisinproteinqualitycontrol.NatRevMolCellBiol.2011Mar;12(3):152-62.doi:10.1038/nrm3065.Epub2011Feb16.PMID:21326199.
29. HaffnerC.TheemergingroleoftheHTRA1proteaseinbrainmicrovasculardisease.FrontDement.2023Apr12;2:1146055.doi:10.3389/frdem.2023.1146055.PMID:39081996;PMCID:PMC11285548.
30. PoepselsS,SprengelA,SaccaB,KaschaniF,KaiserM,GatsogiannisC,RaunserS,ClausenT,EhrmannM.DeterminantsofamyloidfibrildegradationbythePDZproteaseHTRA1.NatChemBiol.2015Nov;11(11):862-9.doi:10.1038/nchembio.1931.Epub2015Oct5.PMID:26436840.
31. XuY,WangS,HuQ,GaoS,MaX,ZhangW,ShenY,ChenF,LaiL,PeiJ.CavityPlus:awebserverforprotein-cavitydetectionwithpharmacophoremodelling,allostericsiteidentificationandcovalentligandbindingabilityprediction.NucleicAcidsRes.2018Jul24;46(W1):W374-W379.doi:10.1093/nar/gky380.PMID:29750256;PMCID:PMC6031032.
32. KochnevY,DurrantJD.FPocketWeb:proteinpocket huntinginaweb browser.JCheminform.2022Aug26;14(1):58.doi:10.1186/s13321-022-00637-0.PMID:36008829;PMCID:PMC9414105.
33. LeGuillouxV,SchmidtkeP,TufferyP.FPocket:anopensourceplatformforligandpocketdetection.BMCBioinformatics.2009Jun2;10:168.doi:10.1186/1471-2105-10-168.PMID:19486540;PMCID:PMC2700099.
34. JendeleL,KrivakR,SkodaP,NovotnyM,HokszaD.PrankWeb:awebserverforligandbindingsitepredictionandvisualization.NucleicAcidsRes.2019Jul2;47(W1):W345-W349.doi:10.1093/nar/gkz424.PMID:31114880;PMCID:PMC6602436.
35. KrivákR,HokszaD.P2Rank:machinelearningbasedtoolforrapidandaccuratepredictionofligandbindingsitesfromproteinstructure.JCheminform.2018Aug14;10(1):39.doi:10.1186/s13321-018-0285-8.PMID:30109435;PMCID:PMC6091426.
36. KoesDR,CamachoCJ.PocketQuery:protein-proteininteractioninhibitorstartingpointsfromprotein-proteininteractionstructure.NucleicAcidsRes.2012Jul;40(WebServerissue):W387-92.doi:10.1093/nar/gks336.Epub2012Apr20.PMID:22523085;PMCID:PMC3394328.
37. KoesDR,CamachoCJ.ZINCPharmer:pharmacophoresearchoftheZINCdatabase.NucleicAcidsRes.2012Jul;40(WebServerissue):W409-14.doi:10.1093/nar/gks378.Epub2012May2.PMID:22553363;PMCID:PMC3394271.
38. Bitencourt-FerreiraG,deAzevedoWFJr.DockingwithSwissDock.MethodsMolBiol.2019;2053:189-202.doi:10.1007/978-1-4939-9752-7_12.PMID:31452106.
39. DainaA,MichielinO,ZoeteVSwissADME:afreewebtoolevaluatepharmacokinetics,drug-likenessandmedicinalchemistryfriendlinessofsmallmolecules.SciRep.2017Mar3;7:42717.doi:10.1038/srep42717.PMID:28256516;PMCID:PMC5335600.
40. RoskoskiR Jr.PropertiesofFDA-approved smallmoleculeprotein kinaseinhibitors:A2024update.PharmacolRes.2024Feb;200:107059.doi:10.1016/j.phrs.2024.107059.Epub2024Jan11.PMID:38216005.
41. MengF,XiY,HuangJ,AyersPW.Acurateddiverse molecular database of blood-brain barrier permeability with chemical descriptors.SciData.2021Oct29;8(1):289.doi:10.1038/s41597-021-01069-5.PMID:34716354;PMCID:PMC8556334.